

Phenotypic landscape inference reveals multiple evolutionary paths to C₄ photosynthesis

Ben P Williams^{1†}, Iain G Johnston^{2†}, Sarah Covshoff¹, Julian M Hibberd^{1*}

¹Department of Plant Sciences, University of Cambridge, Cambridge, United Kingdom;

²Department of Mathematics, Imperial College London, London, United Kingdom

Abstract C₄ photosynthesis has independently evolved from the ancestral C₃ pathway in at least 60 plant lineages, but, as with other complex traits, how it evolved is unclear. Here we show that the polyphyletic appearance of C₄ photosynthesis is associated with diverse and flexible evolutionary paths that group into four major trajectories. We conducted a meta-analysis of 18 lineages containing species that use C₃, C₄, or intermediate C₃–C₄ forms of photosynthesis to parameterise a 16-dimensional phenotypic landscape. We then developed and experimentally verified a novel Bayesian approach based on a hidden Markov model that predicts how the C₄ phenotype evolved. The alternative evolutionary histories underlying the appearance of C₄ photosynthesis were determined by ancestral lineage and initial phenotypic alterations unrelated to photosynthesis. We conclude that the order of C₄ trait acquisition is flexible and driven by non-photosynthetic drivers. This flexibility will have facilitated the convergent evolution of this complex trait.

DOI: [10.7554/eLife.00961.001](https://doi.org/10.7554/eLife.00961.001)

Introduction

The convergent evolution of complex traits is surprisingly common, with examples including camera-like eyes of cephalopods, vertebrates, and cnidaria (Kozmik *et al.*, 2008), mimicry in invertebrates and vertebrates (Santos *et al.*, 2003; Wilson *et al.*, 2012) and the different photosynthetic machineries of plants (Sage *et al.*, 2011a). While the polyphyletic origin of simple traits (Hill *et al.*, 2006; Steiner *et al.*, 2009) is underpinned by flexibility in the underlying molecular mechanisms, the extent to which this applies to complex traits is less clear. C₄ photosynthesis is both highly complex, involving alterations to leaf anatomy, cellular ultrastructure, and photosynthetic metabolism, and also convergent, being found in at least 60 independent lineages of angiosperms (Sage *et al.*, 2011a). As the emergence of the entire C₄ phenotype cannot be comprehensively explored experimentally, C₄ photosynthesis is an ideal system for the mathematical modelling of complex trait evolution as transitions on an underlying phenotype landscape. Furthermore, understanding the evolutionary events that have generated C₄ photosynthesis on many independent occasions has the potential to inform approaches being undertaken to engineer C₄ photosynthesis into C₃ crop species (Hibberd *et al.*, 2008).

The C₄ pathway is estimated to have first evolved between 32 and 25 million years ago (Christin *et al.*, 2011b) in response to multiple ecological drivers, including decreasing atmospheric CO₂ concentration (Vicentini *et al.*, 2008). C₄ species have since radiated to represent the most productive crops and native vegetation on the planet because modifications to their leaves increase the efficiency of photosynthesis in the sub-tropics and tropics (Edwards *et al.*, 2010). In C₄ plants, photosynthetic efficiency is improved compared with C₃ species because significant alterations to leaf anatomy, cell biology and biochemistry lead to higher concentrations of CO₂ around the primary carboxylase RuBisCO (Slack and Hatch, 1967; Langdale, 2011). The morphology of C₄ leaves is typically modified into so-called Kranz anatomy that consists of repeating units of vein, bundle sheath (BS) and mesophyll (M) cells (Hattersley, 1984; Langdale, 2011) (Figure 1—figure supplement 1). Photosynthetic metabolism

*For correspondence: Julian Hibberd@plantsci.cam.ac.uk

†These authors contributed equally to this work

Competing interests: The authors declare that no competing interests exist.

Funding: See page 16

Received: 20 May 2013

Accepted: 05 August 2013

Published: 28 September 2013

Reviewing editor: Dominique Bergmann, Stanford University, United States

© Copyright Williams *et al.* This article is distributed under the terms of the [Creative Commons Attribution License](https://creativecommons.org/licenses/by/4.0/), which permits unrestricted use and redistribution provided that the original author and source are credited.

eLife digest Plants rely on carbon for their growth and survival: in a process called photosynthesis, they use energy from sunlight to convert carbon dioxide and water into carbohydrates and oxygen gas. The chemical reactions that make up photosynthesis are powered by a chain of enzymes, and plants must ensure that these enzymes—which are in the leaves of the plant—are supplied with enough carbon dioxide and water. Carbon dioxide from the atmosphere enters plants through pores in their leaves, but water must be carried up the plant from the roots.

The type of photosynthesis used by about 90% of flowering plant species—including tomatoes and rice—is called C₃ photosynthesis. The first step in this process begins with an enzyme called RuBisCO, which reacts with carbon dioxide and a substance called RuBP to form molecules that contain three carbon atoms (hence the name C₃ photosynthesis).

In a hot climate, however, a plant can lose a lot of water through the pores in its leaves: closing these pores allows the plant to retain water, but this also reduces the supply of carbon dioxide. Under these circumstances this causes problems because RuBisCO uses oxygen to break down RuBP, instead of creating sugars, when carbon dioxide is not readily available. To prevent this process, which wastes a lot of energy and resources, some plants—including maize, sugar cane and many other agricultural staples—have evolved an alternative process called C₄ photosynthesis. Although it is more complex than C₃ photosynthesis, and required many changes to be made to the structure of leaves, C₄ photosynthesis has evolved on more than 60 different occasions.

In C₄ plants, the mesophyll—the region that is associated with the capture of carbon dioxide by RuBisCO in C₃ plants—contains high levels of an alternative enzyme called PEPC that converts carbon dioxide molecules into an acid that contains four carbon atoms. To avoid carbon dioxide being captured by both enzymes, C₄ plants evolved to relocate RuBisCO from the mesophyll to a second set of cells in an airtight structure known as the bundle sheath. The four-carbon acids produced by PEPC diffuse to the cells in the bundle sheath, where they are broken down into carbon dioxide molecules, and photosynthesis then proceeds as normal. This process allows photosynthesis to continue when the level of carbon dioxide in the leaf is low because the plant has closed its pores to retain water.

Since C₄ plants grow faster than C₃ plants, and also require less water, plant biologists would like to introduce certain C₄ traits into C₃ crop plants. To help with this process, Williams, Johnston et al. have used computational methods to explore how C₄ photosynthesis evolved from ancestral C₃ plants. This involved investigating the prevalence of 16 traits that are common to C₄ plants in a total of 73 species that undergo C₃ or C₄ photosynthesis (including 37 species that possess characteristics of both C₃ and C₄).

Williams, Johnston et al. then went on to produce a new mathematical model that represents evolutionary processes as pathways across a multi-dimensional “landscape”. The model shows that traits can be acquired in various orders, and that C₄ photosynthesis evolved through a number of independent pathways. Some traits that evolved early in the transitions to C₄ photosynthesis influenced how evolution proceeded, providing “foundations” upon which further changes evolved.

Interestingly, the structure of the leaf itself appeared to change before any of the photosynthetic enzymes changed. This led Williams, Johnston et al. to conclude that climate change—in particular, the declines in carbon dioxide levels that occurred in prehistoric times—was probably not responsible for the original evolution of C₄ photosynthesis. Nevertheless, these results could help with efforts to adapt important C₃ crop plants to on-going changes in our climate.

DOI: [10.7554/eLife.00961.002](https://doi.org/10.7554/eLife.00961.002)

becomes modified and compartmentalised between the M and BS, with M cells lacking RuBisCO but instead containing high activities of the alternate carboxylase PEPC to generate C₄ acids. The diffusion of these acids followed by their decarboxylation in BS cells around RuBisCO increases CO₂ supply and therefore photosynthetic efficiency (Zhu et al., 2008). C₄ acids are decarboxylated by at least one of three enzymes within BS cells: NADP- or NAD-dependent malic enzymes (NADP-ME or NAD-ME respectively), or phosphoenolpyruvate carboxykinase (PCK) (Hatch et al., 1975). Specific lineages of C₄ species have typically been classified into one of three sub-types, based on the activity of these decarboxylases, as well as anatomical and cellular traits that consistently correlate with each other (Furbank, 2011).

The genetic mechanisms underlying the evolution of cell-specific gene expression associated with the separation of photosynthetic metabolism between M and BS cells involve both alterations to *cis*-elements and *trans*-acting factors (Akyildiz et al., 2007; Brown et al., 2011; Kajala et al., 2012; Williams et al., 2012). Phylogenetically independent lineages of C₄ plants have co-opted homologous mechanisms to generate cell specificity (Brown et al., 2011) as well as the altered allosteric regulation of C₄ enzymes (Christin et al., 2007) indicating that parallel evolution underpins at least part of the convergent C₄ syndrome. However, while a substantial amount of work has addressed the molecular alterations that generate the biochemical differences between C₃ and C₄ plants (Williams et al., 2012) much less is known about the order and flexibility with which phenotypic traits important for C₄ photosynthesis are acquired (Sage et al., 2012). Clues to this question exist in the form of C₃–C₄ intermediates, species exhibiting characteristics of both C₃ or C₄ photosynthesis, such as the activity or localisation of C₄ cycle enzymes (Hattersley and Stone, 1986), the possession of one or more anatomical or cellular adaptations associated with C₄ photosynthesis (Moore et al., 1987), or combinations of both (e.g., Kennedy et al., 1980; Kotayeva et al., 2010). To address these unknown aspects of C₄ evolutionary history, we combined the concept of considering evolutionary paths as stochastic processes on complex adaptive landscapes (Wright, 1932; Gavrilets, 1997) with the analysis of extant C₃–C₄ intermediate species to develop a predictive model of how the full C₄ phenotype evolved.

Results

A meta-analysis of photosynthetic phenotypes

To parameterise the phenotypic landscape underlying photosynthetic phenotypes, data was consolidated from 43 studies encompassing 18 C₃, 18 C₄, and 37 C₃–C₄ intermediate species from 22 genera (Table 1). These C₃–C₄ species are from 18 independent lineages likely representing 18 distinct evolutionary origins of C₃–C₄ intermediacy (Sage et al., 2011a) (Figure 1—figure supplement 2). These studies were used to quantify 16 biochemical, anatomical, and cellular characteristics associated with C₄ photosynthesis (Figure 1—source data 1). Principal components analysis (PCA) was performed to confirm the phenotypic intermediacy of the C₃–C₄ species (Figure 1A). This result, the sister-group relationships of C₃–C₄ species with congeneric C₄ clades (McKown et al., 2005; Vogan et al., 2007; Christin et al., 2011a; Sage et al., 2011a; Khoshravesh et al., 2012) and the prevalence of extant C₃–C₄ species in genera with the most recent origins of C₄ photosynthesis (Christin et al., 2011b) all support the notion that C₃–C₄ species represent phenotypic states through which transitions to C₄ photosynthesis could occur. The combined traits of C₃–C₄ intermediate species therefore represent samples from across the space of phenotypes connecting C₃ to C₄ photosynthesis (Figure 1B). Within our meta-analysis data, C₃–C₄ phenotypes were available for 33 eudicot and 4 monocot species. 16 and 17 of these species have extant congeneric relatives performing NADP-ME or NAD-ME sub-type C₄ photosynthesis respectively. No C₃–C₄ relatives of PCK sub-type C₄ species are known (Sage et al., 2011a). Our meta-analysis therefore encompassed a variety of taxonomic lineages, as well as representing close relatives of known phenotypic variants performing C₄ photosynthesis.

We defined each C₄ trait as either being absent (0) or present (1). For quantitative traits the expectation-maximization (EM) algorithm and hierarchical clustering were used to impartially assign binary scores (Figure 1—figure supplement 3). This generated a 16-bit string for each of the species (Figure 1—source data 1), with a presence or absence score for each of the traits included in our meta-analysis. This defined a 16-dimensional phenotype space with 2¹⁶ (65,536) nodes corresponding to all possible combinations of presence (1) and absence (0) scores for each characteristic.

A novel Bayesian approach for predicting evolutionary trajectories

Many existing methods of inference for evolutionary trajectories rely on phylogenetic information or assumptions about the fitness landscape underlying evolutionary dynamics (Weinreich et al., 2005; Lobkovsky et al., 2011; Mooers and Heard, 2013). In convergent evolution, these properties are not always known, as convergent lineages may be genetically distant and associated with poor phylogenetic reconstructions. In addition, the selective pressures experienced by each may be different and dynamic. We therefore consider the convergent evolution of C₄ fundamentally as the acquisition of the key phenotypic traits identified through our meta-analysis (Figure 1B). The process of acquisition of these traits can be pictured as a path on the 16-dimensional hypercube (Figure 1C), from the node labelled with all 0's (the C₃ phenotype, with no C₄ characteristics) to the node labelled with all 1's (the C₄ phenotype, with all C₄ characteristics).

Table 1. Summary of C₃–C₄ lineages assessed

Family	Species	References*
Amaranthaceae	<i>Alternanthera ficoides</i> (C ₃ –C ₄)	Rajendrudu et al. (1986)
	<i>Alternanthera tenella</i> (C ₃ –C ₄)	Devi and Raghavendra (1993)
	<i>Alternanthera pungens</i> (C ₄)	Devi et al. (1995)
Asteraceae	<i>Flaveria cronquistii</i> (C ₃)	
	<i>Flaveria pringlei</i> (C ₃)	
	<i>Flaveria robusta</i> (C ₃)	
	<i>Flaveria angustifolia</i> (C ₃ –C ₄)	
	<i>Flaveria anomala</i> (C ₃ –C ₄)	Ku et al. (1983)
	<i>Flaveria chloraefolia</i> (C ₃ –C ₄)	Holaday et al. (1984)
	<i>Flaveria floridana</i> (C ₃ –C ₄)	Adams et al. (1986)
	<i>Flaveria linearis</i> (C ₃ –C ₄)	Brown and Hattersley (1989)
	<i>Flaveria oppositifolia</i> (C ₃ –C ₄)	Ku et al. (1991)
	<i>Flaveria ramosissima</i> (C ₃ –C ₄)	Rosche et al. (1994)
	<i>Flaveria sonorensis</i> (C ₃ –C ₄)	Casati et al. (1999)
	<i>Flaveria brownie</i> (C ₃ –C ₄)	McKown et al. (2005)
	<i>Flaveria vaginata</i> (C ₃ –C ₄)	McKown and Dengler (2007)
	<i>Flaveria pubescens</i> (C ₃ –C ₄)	Gowik et al. (2011)
	<i>Flaveria australasica</i> (C ₄)	
	<i>Flaveria bidentis</i> (C ₄)	
	<i>Flaveria kochiana</i> (C ₄)	
<i>Flaveria trinervia</i> (C ₄)		
	<i>Parthenium incanum</i> (C ₃)	Moore et al. (1987)
	<i>Parthenium hysterophorus</i> (C ₃ –C ₄)	Devi and Raghavendra (1993)
Boraginaceae	<i>Heliotropium europaeum</i> (C ₃)	
	<i>Heliotropium calcicola</i> (C ₃)	Vogan et al. (2007)
	<i>Heliotropium convolvulaceum</i> (C ₃ –C ₄)	Muhaidat et al. (2011)
	<i>Heliotropium greggii</i> (C ₃ –C ₄)	
	<i>Heliotropium polyphyllum</i> (C ₄)	
Brassicaceae	<i>Moricandia foetida</i> (C ₃)	Holaday et al. (1981)
	<i>Moricandia arvensis</i> (C ₃ –C ₄)	Rawsthorne et al. (1988)
	<i>Moricandia spinosa</i> (C ₃ –C ₄)	Beebe and Evert (1990)
	<i>Moricandia nitens</i> (C ₃ –C ₄)	Rawsthorne et al. (1998)
	<i>Raphanus sativus</i> (C ₃)	Ueno et al. (2003)
	<i>Diplotaxis muralis</i> (C ₃ –C ₄)	Ueno et al. (2006)
	<i>Diplotaxis tenuifolia</i> (C ₃ –C ₄)	
Chenopodiaceae	<i>Salsola oreophila</i> (C ₃)	P'yankov et al. (1997)
	<i>Salsola arbusculiformis</i> (C ₃ –C ₄)	Voznesenskaya et al. (2001)
	<i>Salsola arbuscula</i> (C ₄)	
Cleomaceae	<i>Cleome spinosa</i> (C ₃)	Voznesenskaya et al. (2007)
	<i>Cleome paradoxa</i> (C ₃ –C ₄)	Koteyeva et al. (2010)
	<i>Cleome gynandra</i> (C ₄)	
Cyperaceae	<i>Eleocharis acuta</i> (C ₃)	Bruhl and Perry (1995)
	<i>Eleocharis acicularis</i> (C ₃ –C ₄)	Keeley (1999)
	<i>Eleocharis tetragona</i> (C ₄)	

Table 1. Continued on next page

Table 1. Continued

Family	Species	References*		
Euphorbiaceae	<i>Euphorbia angusta</i> (C ₃)	Sage et al. (2011b)		
	<i>Euphorbia acuta</i> (C ₃ –C ₄)			
	<i>Euphorbia lata</i> (C ₃ –C ₄)			
	<i>Euphorbia mesembryanthemifolia</i> (C ₄)			
Molluginaceae	<i>Mollugo tenella</i> (C ₃)	Sayre et al. (1979) Kennedy et al. (1980) Christin et al. (2011a)		
	<i>Mollugo verticillata</i> (C ₃ –C ₄)			
	<i>Mollugo naudicalis</i> (C ₃ –C ₄)			
	<i>Mollugo pentaphylla</i> (C ₃ –C ₄)			
	<i>Mollugo cerviana</i> (C ₄)			
Poaceae	<i>Avena sativa</i> (C ₃)	Slack and Hatch (1967) Hattersley and Stone (1986) Brown and Hattersley (1989) Goldstein et al. (1976) Ku et al. (1976) Ku and Edwards (1978) Rathnam and Chollet (1978) Rathnam and Chollet (1979) Holaday and Black (1981) Hattersley (1984) Slack and Hatch (1967) Slack and Hatch (1967) Slack and Hatch (1967) Slack and Hatch (1967)		
	<i>Neurachne tenuifolia</i> (C ₃)			
	<i>Neurachne minor</i> (C ₃ –C ₄)			
	<i>Neurachne munroi</i> (C ₄)			
	<i>Panicum bisculatum</i> (C ₃)			
	<i>Panicum hians</i> (C ₃ –C ₄)			
	<i>Panicum milioides</i> (C ₃ –C ₄)			
	<i>Panicum miliaceum</i> (C ₄)			
	<i>Saccharum officinarum</i> (C ₄)			
	<i>Sorghum bicolor</i> (C ₄)			
	<i>Triticum aestivum</i> (C ₃)			
	<i>Zea mays</i> (C ₄)			
	Portulacaceae		<i>Sesuvium portulacastrum</i> (C ₃)	Voznesenskaya et al. (2010)
			<i>Portulaca cryptopetala</i> (C ₃ –C ₄)	
<i>Portulaca oleracea</i> (C ₄)				
Scrophularaceae	<i>Anticharis kaokoensis</i> (C ₃)	Khoshravesh et al. (2012)		
	<i>Anticharis ebracteata</i> (C ₃ –C ₄)			
	<i>Anticharis imbricate</i> (C ₃ –C ₄)			
	<i>Anticharis namibensis</i> (C ₃ –C ₄)			
	<i>Anticharis glandulosa</i> (C ₄)			

The family, species, photosynthetic type and original study are listed. In total, 16 characteristics relating to C₄ photosynthesis were extracted from 43 studies encompassing 18 C₃, 18 C₄, and 37 C₃–C₄ intermediate species.

*References apply to all species within each genus.

DOI: [10.7554/eLife.00961.003](https://doi.org/10.7554/eLife.00961.003)

The phenotypic landscape underlying the evolution of C₄ photosynthesis was then modelled as a transition network, with weighted edges describing the probability of transitions occurring between two phenotypic states (two nodes on the hypercube, **Figure 1—figure supplement 4**). Observed intermediate points were then used to constrain the structure of these phenotypic landscapes. To do this, we developed inferential machinery based on the framework of Hidden Markov Models (HMMs) (**Rabiner, 1989**) (**Figure 1—figure supplement 4**) and simulated an ensemble of Markov chains on trial transition networks. Each of these chains represents a possible evolutionary pathway from C₃ to C₄, and passes through several intermediate phenotypic states. The likelihood of observing intermediate states with characteristics compatible with the biologically observed data on C₃–C₄ intermediates was recorded for the set of paths supported on each trial network. A Bayesian MCMC procedure was used

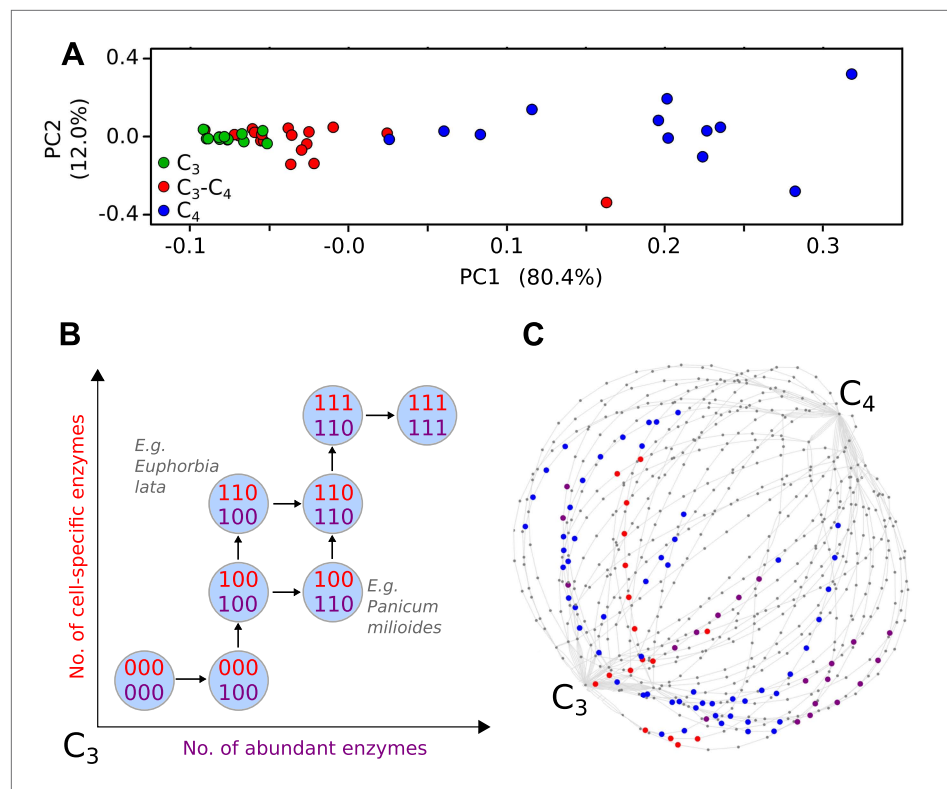


Figure 1. Evolutionary paths to C_4 phenotype space modelled from a meta-analysis of C_3 - C_4 phenotypes. Principal component analysis (PCA) on data for the activity of five C_4 cycle enzymes confirms the intermediacy of C_3 - C_4 species between C_3 and C_4 phenotype spaces (**A**). Each C_4 trait was considered absent in C_3 species and present in C_4 species, with previously studied C_3 - C_4 intermediate species representing samples from across the phenotype space (**B**). With a dataset of 16 phenotypic traits, a 16-dimensional space was defined. (**C**) A 2D representation of 50 pathways across this space. The phenotypes of multiple C_3 - C_4 species were used to identify pathways compatible with individual species (e.g., *Alternanthera ficoides* [red nodes] and *Parthenium hysterophorus* [blue nodes]), and pathways compatible with the phenotypes of multiple species (purple nodes).

DOI: [10.7554/eLife.00961.004](https://doi.org/10.7554/eLife.00961.004)

The following source data and figure supplements are available for figure 1:

Source data 1. Binary scoring of C_4 traits present in C_3 - C_4 species.

DOI: [10.7554/eLife.00961.005](https://doi.org/10.7554/eLife.00961.005)

Figure supplement 1. A graphical representation of key phenotypic changes distinguishing C_3 and C_4 leaves.

DOI: [10.7554/eLife.00961.006](https://doi.org/10.7554/eLife.00961.006)

Figure supplement 2. Phylogenetic distribution of C_4 and C_3 - C_4 lineages across the angiosperm phylogeny.

DOI: [10.7554/eLife.00961.007](https://doi.org/10.7554/eLife.00961.007)

Figure supplement 3. Clustering quantitative traits by EM algorithm and hierarchical clustering.

DOI: [10.7554/eLife.00961.008](https://doi.org/10.7554/eLife.00961.008)

Figure supplement 4. Illustration of the principle by which evolutionary pathways emit intermediate signals.

DOI: [10.7554/eLife.00961.009](https://doi.org/10.7554/eLife.00961.009)

to sample from the set of networks most compatible with the meta-analysis dataset, and thus most likely to represent the underlying dynamics of C_4 evolution. The order in which phenotypic characteristics were acquired was recorded for paths on each network compatible with the C_3 - C_4 species data, and posterior probability distributions (given uninformative priors) for the time-ordered acquisition of each C_4 trait were generated. For further information and mathematical details, see 'Methods'.

To model the evolutionary paths generating C_4 without requiring additional dimensionality, we imposed that only one C_4 trait may be acquired at a time, and loss of acquired C_4 traits was forbidden. To test if we were nevertheless able to detect traits acquired simultaneously in evolution, we tested our approach on artificial positive control datasets containing intermediate nodes representing a step-wise evolutionary sequence of events (**Figure 2A**) and an evolutionary pathway in which four traits are

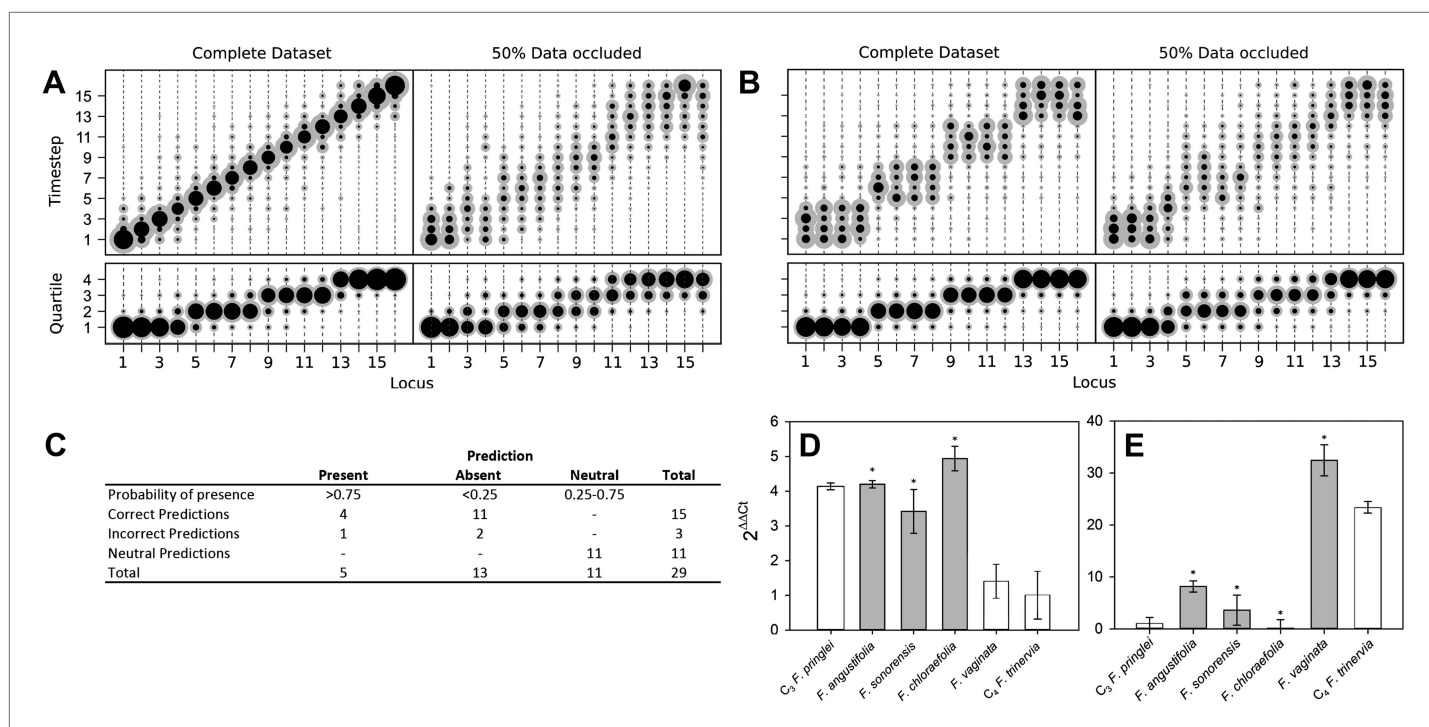


Figure 2. Verifying a novel Bayesian approach for predicting evolutionary trajectories. (**A** and **B**) Datasets were obtained from an artificially constructed diagonal dynamic matrix (**A**), and a diagonal matrix with linked timing of locus acquisitions (**B**). The single, diagonal evolutionary trajectory was clearly replicated in both examples, over a time-scale of 16 individual steps, or four coarse-grained quartiles. We subjected these artificial datasets to our inferential machinery with fully characterised artificial species, and with 50% of data occluded in order to replicate the proportion of missing data from our C₃–C₄ dataset. (**C**) When applied to our meta-analysis of C₃–C₄ data, predictions were generated for every trait missing from the biological dataset. We tested this predictive machinery by generating 29 artificial datasets, each missing one data point, and comparing the presence/absence of the trait as predicted by our approach with the experimental data from the original study. (**D** and **E**) Quantitative real-time PCR (qPCR) was used to verify the predicted phenotypes of four C₃–C₄ species. The abundance *RbcS* (**D**) and *MDH* (**E**) transcripts were determined from six *Flaveria* species. White bars represent phenotypes already determined by other studies, grey bars those that were predicted by the model and asterisks denote intermediate species phenotypes correctly predicted by our approach (Error bars indicate SEM, N = 3).

DOI: 10.7554/eLife.00961.010

The following figure supplements are available for figure 2:

Figure supplement 1. Computational prediction of C₃–C₄ intermediate phenotypes.

DOI: 10.7554/eLife.00961.011

acquired simultaneously at a time (**Figure 2B**). Our approach clearly assigned equal acquisition probabilities to traits whose timing was linked in the underlying dataset, even when 50% of the data was occluded (**Figure 2B**). These data are consistent with this approach detecting the simultaneous acquisition of traits in evolution, even though single-trait acquisitions are simulated.

Verifying prediction accuracy

The presence and absence of unknown phenotypes were predicted by recording all phenotypes encountered along a set of simulated evolutionary trajectories that were compatible with the data from a given species (**Figure 1—figure supplement 4**), and calculating the posterior distribution of the proportion of these phenotypes with the value 1 for the unknown trait. If the mean of this distribution was <25% or >75%, and that value fell outside one standard deviation of the mean, the missing trait was assigned a strong prediction of absence or presence. To comprehensively test the accuracy of our predictive machinery, we generated 29 occluded datasets, consisting of the original full dataset with one randomly chosen data point removed. The predicted phenotype of each missing trait was then compared with the known phenotype published in the original study. For 29 occluded traits 18 were strongly predicted to be present or absent, and the remaining 11 predictions were neutral. Of the 18 strongly predicted traits (i.e., <25% or >75% probability), 15 were correct, with only one false positive and two false negative predictions (**Figure 2C**). The approach therefore assigns neutral predictions much more frequently than

false positive or false negative predictions, suggesting that its outputs are highly conservative, and thus unlikely to produce artefacts. Predictions were generated for phenotypes that have not yet been described in C_3 – C_4 species (**Figure 2—figure supplement 1**). Quantitative real-time PCR experimentally verified a subset of these, relating to abundance of C_4 enzymes not previously measured (**Figure 2D–E**). We also found that the model was able to successfully infer evolutionary dynamics in artificially constructed datasets (**Figure 2A–B**). Taken together, these prediction and verification studies illustrate that our approach robustly identifies key features of C_4 evolution.

A high-resolution model for the evolutionary events generating C_4

The posterior probability distributions for the acquisition time of each phenotypic trait were combined to produce an objective, computationally generated blueprint for the order of evolutionary events generating C_4 photosynthesis (**Figure 3**). These results were consistent with previous work on subsets of C_4 lineages that proposed the BS-specificity of GDC occurs prior to the evolution of C_4 metabolism (*Hylton et al., 1988; Rawsthorne et al., 1988; Devi et al., 1995; Sage et al., 2012*),

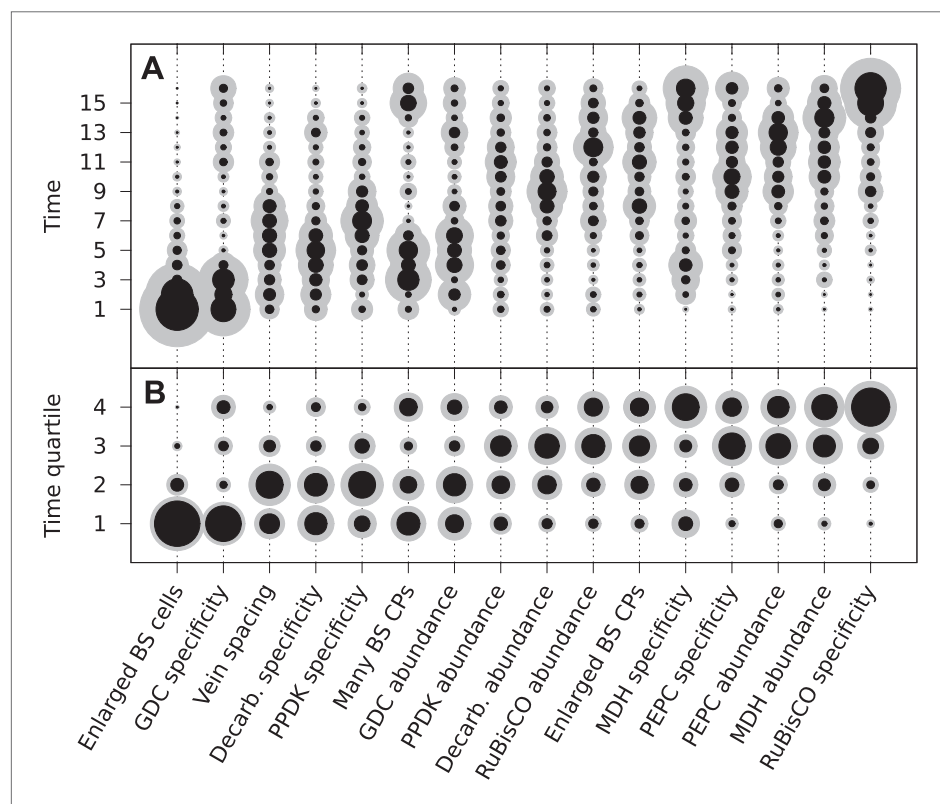


Figure 3. The mean ordering of phenotypic changes generating C_4 photosynthesis. EM-clustered data from C_3 – C_4 intermediate species were used to generate posterior probability distributions for the timing of the acquisition of C_4 traits in sixteen evolutionary steps (**A**) or four quartiles (**B**). Circle diameter denotes the mean posterior probability of a trait being acquired at each step in C_4 evolution (the Bayes estimator for the acquisition probability). Halos denote the standard deviation of the posterior. The 16 traits are ordered from left to right by their probability of being acquired early to late in C_4 evolution. Abbreviations: bundle sheath (BS), glycine decarboxylase (GDC), chloroplasts (CPs), decarboxylase (Decarb.), pyruvate, orthophosphate dikinase (PPDK), malate dehydrogenase (MDH), phosphoenolpyruvate carboxylase (PEPC).

DOI: [10.7554/eLife.00961.012](https://doi.org/10.7554/eLife.00961.012)

The following figure supplements are available for figure 3:

Figure supplement 1. Results obtained using data clustered by hierarchical clustering.

DOI: [10.7554/eLife.00961.013](https://doi.org/10.7554/eLife.00961.013)

Figure supplement 2. Adding or removing traits does not affect the predicted order of evolutionary events.

DOI: [10.7554/eLife.00961.014](https://doi.org/10.7554/eLife.00961.014)

Figure supplement 3. Probabilities of C_4 traits being acquired simultaneously.

DOI: [10.7554/eLife.00961.015](https://doi.org/10.7554/eLife.00961.015)

and loss of RuBisCO from M cells occurs late (*Cheng et al., 1988; Khoshravesh et al., 2012*), but also provided higher resolution insight into the order of events generating C₄ metabolism. Alterations to leaf anatomy as well as cell-specificity and increased abundance of multiple C₄ cycle enzymes were predicted to evolve prior to any alteration to the primary C₃ and C₄ photosynthetic enzymes RuBisCO and phosphoenolpyruvate carboxylase (PEPC) (*Figure 3*).

There was also strong evidence for enlargement of BS cells as an early innovation in most C₄ lineages (*Figure 3*), consistent with the suggestion that this was an ancestral state within C₃ ancestors of C₄ grass lineages and that this contributed to the high number of C₄ origins within this family (*Christin et al., 2013; Griffiths et al., 2013*). The compartmentation of PEPC into M cells and its increased abundance compared with C₃ leaves was predicted to occur at similar times, but for all other C₄ enzymes the evolution of increased abundance and cellular compartmentation were clearly separated by the acquisition of other traits (*Figure 3*). This result is consistent with molecular analysis of genes encoding C₄ enzymes that indicates cell-specificity and increased expression are mediated by different *cis*-elements (*Akyildiz et al., 2007; Kajala et al., 2012; Wiludda et al., 2012*).

Two approaches were taken to verify that these conclusions are robust and accurately reflect biological data. First, the analysis was repeated using scores for presence or absence of traits that were assigned by hierarchical clustering, as opposed to using the EM algorithm (*Figure 3—figure supplement 1A*). Although hierarchical clustering generated differences in the scoring of a small number of traits, the predicted evolutionary trajectories were not affected, producing highly similar results (*Figure 3—figure supplement 1B*). Second, we introduced structural changes to the phenotype space, by both adding and subtracting traits from the analysis (*Figure 3—figure supplement 2*). Removing two independent pairs of traits from the analysis did not affect the predicted timing of the remaining 14 traits (*Figure 3—figure supplement 2A–B*). However, increased standard deviations were observed in some cases (e.g., for the probabilities of acquiring enlarged BS cells, or decreased vein spacing) likely a consequence of using fewer data. To test if the addition of data might also affect the results, we performed an analysis with two additional traits included (*Figure 3—figure supplement 2C*). We selected two traits that have been widely observed in C₃–C₄ species, the centripetal positioning of mitochondria and the centrifugal or centripetal position of chloroplasts within BS cells (*Sage et al., 2012*). Despite the widespread occurrence of these traits, their functional importance remains unclear (*Sage et al., 2012*). Consistent with observations made from several genera, we predict that these cellular alterations are acquired early in the evolution of C₄ photosynthesis (*Hylton et al., 1988; McKown and Dengler, 2007; Muhaidat et al., 2011; Sage et al., 2011b*). Importantly, including these additional early traits in the analysis did not alter the predicted order of the original 16 traits. Together, these analyses did not alter our main conclusions, suggesting that they are robust.

The order of C₄ trait evolution is flexible

In addition to the likely order of evolutionary events generating C₄ photosynthesis, the number of molecular alterations required is also unknown. We therefore aimed to test if multiple traits were predicted to evolve with linked timing, and therefore likely mediated by a single underlying mechanism. To achieve this, we performed a contingency analysis by considering trajectories across phenotype space beginning with a given initial acquisition step. In this analysis, the starting genome had one of the 16 traits acquired and the rest absent, and the contingency of the subsequent trajectory upon the initial step was recorded. This approach was designed to test if acquiring one C₄ trait increased the probability of subsequently acquiring other traits, thus detecting if the evolution of multiple traits is linked by underlying mechanisms. Inflexible linkage between multiple traits was detected in artificial positive control datasets (*Figure 2B*) but not in the C₃–C₄ dataset (*Figure 3—figure supplement 3*). This result suggests that the order of C₄ trait acquisition is flexible. Multiple origins of C₄ may therefore have been facilitated by this flexibility in the evolutionary pathways connecting C₃ and C₄ phenotypes.

C₄ evolved via multiple distinct evolutionary trajectories

Our Bayesian analysis strongly indicates that there are multiple evolutionary pathways by which C₄ traits are acquired by all lineages of C₄ plants. First, no single sequence of acquisitions was capable of producing intermediate phenotypes compatible with all observations ('Methods'). Second, several traits such as compartmentation of GDC into BS and the increased number of chloroplasts in the BS clearly displayed bimodal probability distributions for their acquisition (*Figure 3*). This bimodality is indicative of multiple distinct pathways to C₄ photosynthesis that acquire traits at earlier or later times. To investigate factors

underlying this bimodality, we inferred evolutionary pathways generating the C_4 leaf using data from monocot and eudicot lineages, or from lineages using NAD malic enzyme (NAD-ME) or NADP malic enzyme (NADP-ME) as their primary C_4 acid decarboxylase. PCA on the entire set of inferred transition networks for monocot and dicot subsets revealed distinct separation (**Figure 4A**), suggesting that the topology of the evolutionary landscape surrounding C_4 is largely different for these two anciently diverged taxa. Performing this PCA including networks that were inferred from the full data set (with both lineages) confirmed that this separation is a robust result and involves posterior variation on a

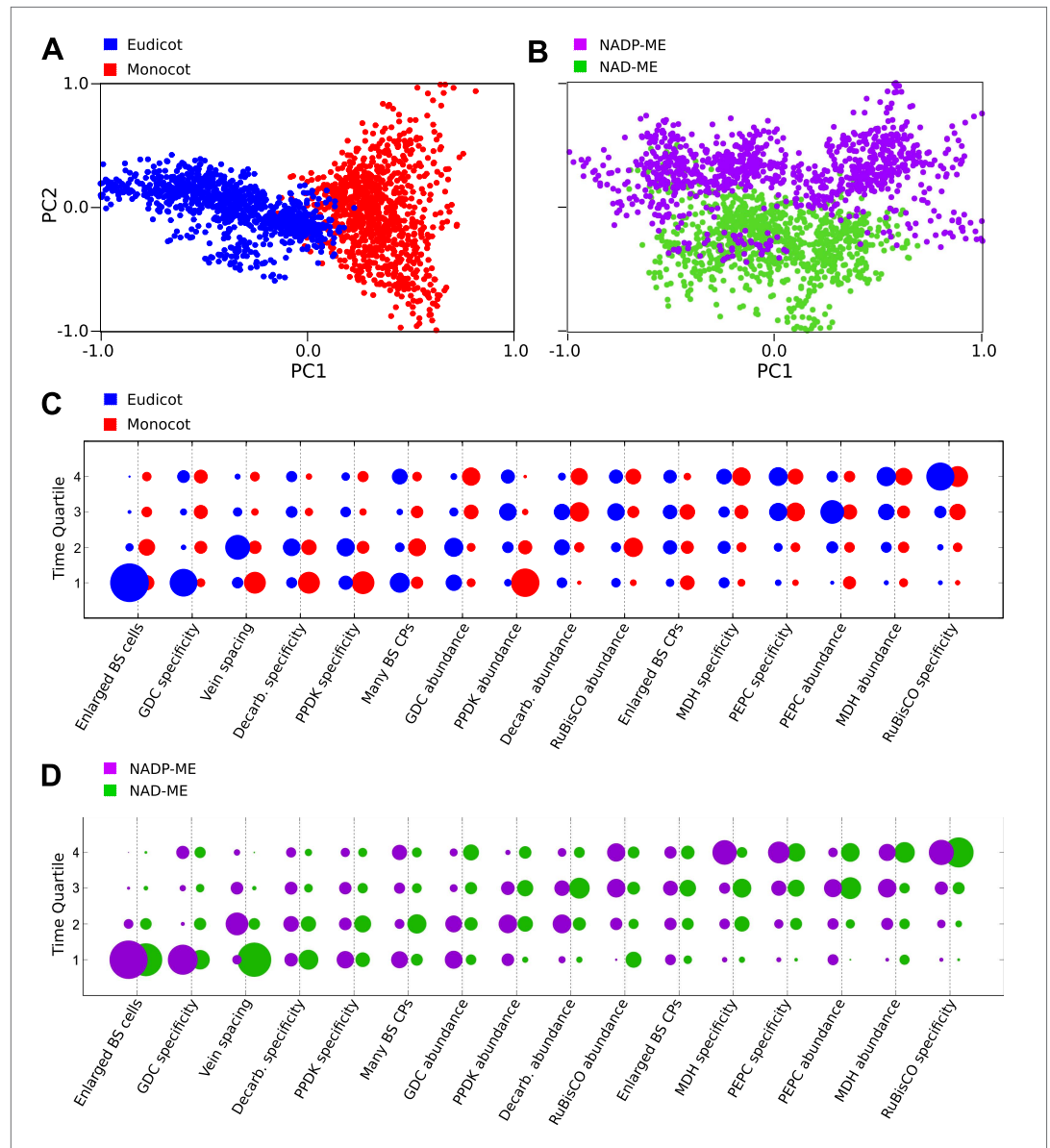


Figure 4. Differences in the evolutionary events generating different C_4 sub-types and distantly related taxa. Principal component analysis (PCA) on the entire landscape of transition probabilities using only monocot and eudicot data (**A**) and data from NADP-ME and NAD-ME sub-type lineages (**B**) shows broad differences between the evolutionary pathways generating C_4 in each taxon. Monocots and eudicots differ in the predicted timing of events generating C_4 anatomy and biochemistry (**C**), whereas NADP-ME and NAD-ME lineages differ primarily in the evolution of decreased vein spacing and greater numbers of chloroplasts in BS cells (**D**).
DOI: [10.7554/eLife.00961.016](https://doi.org/10.7554/eLife.00961.016)

The following figure supplements are available for figure 4:

Figure supplement 1. Variation between lineages compared to variance of overall dataset.
DOI: [10.7554/eLife.00961.017](https://doi.org/10.7554/eLife.00961.017)

comparable scale to that of the full set of possible networks (**Figure 4—figure supplement 1**). Analysis of the posterior probabilities of the mean pathways representing either monocots and dicots revealed that this separation is the result of differences in the timing of events generating both anatomical and biochemical traits (**Figure 4C**). We propose that the ancient divergence of the monocot and eudicot clades constrained the evolution of C_4 photosynthesis to broadly different evolutionary pathways in each.

There was more overlap between the landscapes generating NAD-ME and NADP-ME species (**Figure 4B**), likely reflecting the convergent origins of NAD-ME and NADP-ME sub-types (**Furbank, 2011; Sage et al., 2011a**). Despite the traditional definition of these lineages on the basis of biochemical differences, we detected differences in the timing of their anatomical evolution (**Figure 4D**). For example, in NAD-ME lineages, increased vein density was predicted to be acquired early in C_4 evolution, while in NADP-ME species this trait showed a broadly different trajectory (**Figure 4D**). The proliferation of chloroplasts in the BS was also acquired with different timings between the two sub-types. The alternative evolutionary pathways generating the NADP-ME and NAD-ME subtypes were therefore defined by differences in the timing of anatomical and cellular traits that are predicted to precede the majority of biochemical alterations (**Figure 3, Figure 4D**). We therefore conclude that these distinct sub-types evolved as a consequence of alternative evolutionary histories in response to non-photosynthetic pressures. Furthermore, we propose that early evolutionary events determined the downstream phenotypes of C_4 sub-types by restricting lineages to independent pathways across phenotype space.

Discussion

A novel Bayesian technique for inferring stochastic trajectories

The adaptive landscape metaphor has provided a powerful conceptual framework within which evolutionary transitions can be modelled (**Gavrilets, 1997; Whibley et al., 2006; Lobkovsky et al., 2011**). However, the majority of complex biological traits provide numerous challenges in utilising such an approach, including missing phenotypic data, incomplete phylogenetic information and in the case of convergent evolution, variable ancestral states. Here we report the development of a novel, predictive Bayesian approach that is able to infer likely evolutionary trajectories connecting phenotypes from sparsely sampled, highly stochastic data. With this model, we provided insights into the evolution of one of the most complex traits to have arisen in multiple lineages: C_4 photosynthesis. However, as our approach is not dependent on detailed phylogenetic inference, we propose that it could be used to model the evolution of other complex traits, such as those in the fossil record, which are also currently limited by the fragmented nature of data available (**Kidwell and Holland, 2002**). Our approach is also not limited by the time-scale over which predicted trajectories occur. As a result, it may be useful in inferring pathways underlying stochastic processes occurring over much shorter timescales, such as disease or tumour progression, or the differentiation of cell types.

C_4 evolution was initiated by non-photosynthetic drivers

A central hypothesis for the ecological drivers of C_4 evolution is that declining CO_2 concentration in the Oligocene decreased the rate of carboxylation by RuBisCO, creating a strong pressure to evolve alternative photosynthetic strategies (**Christin et al., 2008; Vicentini et al., 2008**). According to this hypothesis, alterations to the localisation and abundance of the primary carboxylases PEPC and RuBisCO would be expected to occur early in the evolutionary trajectories generating C_4 . Conversely, our data suggest that alterations to anatomy and cell biology were predicted to precede the majority of biochemical alterations, and that other enzymes of the C_4 pathway are recruited prior to PEPC and RuBisCO (**Figure 3**). These enzymes, such as PPKK and C_4 acid decarboxylases, function in processes not related to photosynthesis within leaves of C_3 plants (**Aubry et al., 2011**), so the early changes to abundance and localisation of these enzymes within C_4 lineages may have been driven by non-photosynthetic pressures. A recent *in silico* study also predicts that changes to photorespiratory metabolism and GDC in BS cells evolved prior to the C_4 pathway (**Heckman et al., 2013**). Our model predicts that BS-specificity of GDC was acquired early in C_4 evolution for the majority of lineages. However, we also note that the predicted timing of GDC BS-specificity is bimodal in our analysis (**Figure 3**), and not predicted to be acquired early in monocot lineages (**Figure 4C**). These results suggest that this is not a feature of C_4 evolution to have occurred repeatedly in all lineages.

Recent evidence from physiological and ecological studies has identified a number of additional environmental pressures that may have driven the evolution and radiation of C_4 lineages, including

high evaporative demands (*Osborne and Sack, 2012*) and increased fire frequency (*Edwards et al., 2010*). Increased BS volume and vein density have been proposed as likely adaptations to improve leaf hydraulics under drought (*Osborne and Sack, 2012; Griffiths et al. 2013*), but nothing is known about how early recruitment of GDC, PPDK, and C₄ acid decarboxylases (*Figure 3*) may relate to these pressures. A better understanding of the mechanisms underlying the recruitment of these enzymes (*Brown et al., 2011; Kajala et al., 2012; Wiludda et al., 2012*) may help identify the key molecular events facilitating C₄ evolution.

Our data also suggest that modifications to leaf development drove the evolution of diverse C₄ sub-types. For example, we find that differences in the timing of events altering leaf vascular development and BS chloroplast division occur prior to the appearance of the alternative evolutionary pathways generating the NADP-ME and NAD-ME biochemical sub-types (*Figure 4D*). These traits are predicted to evolve prior to any alterations to the C₄ acid decarboxylase enzymes that traditionally define these sub-types (*Furbank, 2011*). As an homologous mechanism has been shown to regulate the cell-specificity of gene expression in both NADP-ME and NAD-ME gene families in independent lineages (*Brown et al., 2011*), it is unlikely that mechanisms underlying the recruitment of these enzymes drove the evolution of distinct sub-types. We therefore conclude that these different sub-types evolved as a consequence of alternative evolutionary histories in leaf development, rather than biochemical or photosynthetic pressures. This may explain why differences in the carboxylation efficiency or photosynthetic performance of different C₄ sub-types have never been detected (*Furbank, 2011*), making the adaptive significance of different decarboxylation mechanisms difficult to explain. Instead, we propose that early evolutionary events determined the downstream phenotypes of C₄ sub-types by restricting lineages to independent pathways across phenotype space. The numerous differences in leaf development and cell biology between C₄ sub-types (*Furbank, 2011*) may provide clues as to which developmental changes underlie subsequent differences in metabolic evolution.

Convergent evolution was facilitated by flexibility in evolutionary trajectories

C₄ photosynthesis provides an excellent example of how independent lineages with a wide range of ancestral phenotypes can converge upon similar complex traits. Several studies on more simple traits have demonstrated that convergence upon a phenotype can be specified by diverse genotypes, and thus non-homologous molecular mechanisms in independent lineages (*Wittkopp et al., 2003; Hill et al., 2006; Steiner et al., 2009*). Taken together, our data also indicate that flexibility in the viable series of evolutionary events has also facilitated the convergence of this highly complex trait. First, we show that at least four distinct evolutionary trajectories underlie the evolution of C₄ lineages (*Figure 4*). Second, we find no evidence for inflexible linkage between the predicted timing of distinct C₄ traits (*Figure 3—figure supplement 1*). This diversity in viable pathways also helps explain why C₄ has been accessible to such a wide variety of species and not limited to a smaller subset of the angiosperm phylogeny. A recent model for the evolution of the biochemistry associated with the C₄ leaf also found that C₄ photosynthesis was accessible from any surrounding point of a fitness landscape (*Heckman et al., 2013*). Our study of C₄ anatomy, biochemistry, and cell biology also suggests the C₄ phenotype is accessible from multiple trajectories. Encouragingly, the trajectories predicted by *Heckman et al. (2013)* were found to pass through phenotypes of C₃–C₄ species, despite the fact that these species were not used to parameterise the evolutionary landscape. As different mechanisms generate increased abundance and cell-specificity for the majority C₄ enzymes in independent C₄ lineages (reviewed in *Langdale, 2011; Williams et al., 2012*), it is likely that mechanistic diversity underlies the multiple evolutionary pathways generating C₄ photosynthesis and may be a key factor in facilitating the convergent evolution of complex traits. This may benefit efforts to recapitulate the acquisition of C₄ photosynthesis through the genetic engineering of C₃ species (*Hibberd et al., 2008*), expanding the molecular toolbox available to establish C₄ traits in distinct phenotypic backgrounds.

Methods

Biological data from C₄ intermediates

Data from eighteen C₃, seventeen C₄, and thirty-seven C₃–C₄ species were consolidated from 43 studies that have examined the phenotypic characteristics of C₃–C₄ species since their discovery in

1974 (**Table 1**). Values for sixteen of the most widely studied C_3 characteristics were recorded for each intermediate species, as well as congeneric C_3 and C_4 relatives where available. The majority of data on enzyme abundance and the number and size of bundle sheath (BS) chloroplasts were obtained from studies employing the same methodology and were thus cross-comparable (e.g., *Goldstein et al., 1976; Ku et al., 1976; Ku and Edwards, 1978; Sayre et al., 1979; Holaday et al., 1981; Holaday and Black, 1981; Ku et al., 1983; Adams et al., 1986; Rajendrudu et al., 1986; Ku et al., 1991; Devi and Raghavendra, 1993; Bruhl and Perry, 1995; Casati et al., 1999; Keeley, 1999*). These cross-comparable quantitative data were partitioned into presence absence scores using two clustering techniques, the expectation-maximisation (EM) algorithm and hierarchical clustering (**Figure 1—figure supplement 3**). EM clustering was performed using a one-dimensional mixture model with two assigned components (e.g., presence and absence clusters), allowing for variable variance between the two components of the model, and variable population size between the two components. Hierarchical clustering was performed using a complete-linkage agglomerative approach, partitioning clusters by maximum distance according to a Euclidean distance metric. This approach identifies clusters with common variance, thus contrasting with the clusters of variable variance identifiable by EM.

For quantitative data not comparable with other studies (e.g., *Ku and Edwards, 1978; Rathnam and Chollet, 1978; Rathnam and Chollet, 1979; Holaday et al., 1984; Brown and Hattersley, 1989; Beebe and Evert, 1990; P'yankov et al., 1997; Gowik et al., 2011*), values obtained for intermediate species were scored as 1 or 0 if they were closer to the values for the respective C_4 or C_3 controls used in the original study. For qualitative abundance data from immunoblots (e.g., *Rosche et al., 1994; Voznesenskaya et al., 2007; Voznesenskaya, 2010*), relative band intensity was measured using ImageJ software (*Abramoff et al., 2004*) and abundance was scored as 1 or 0 if the band intensity value was closer to the C_4 or C_3 control respectively. For qualitative cell-specificity data from immunolocalisations (e.g. *Voznesenskaya et al., 2001; Ueno et al., 2003, 2006; Muhaidat et al., 2011*), a presence score was only assigned if the enzyme appeared completely absent from either mesophyll (M) or BS cells. We represent the phenotypic properties of each intermediate species as a string of $L = 16$ numbers (**Figure 1—source data 1**). We will refer to these strings as *phenotype strings* of L loci, with each locus describing data on the corresponding phenotypic trait. In a given locus, 0 denotes the absence of a C_4 trait, 1 denotes the presence of a C_4 trait, and 2 denotes missing data.

Principal component analysis (PCA)

PCA was performed on five variables for C_4 cycle enzyme activity, with missing values estimated using the EM algorithm for PCA as described by *Roweis (1998)*.

Model transition networks

The fundamental element underlying our analysis is a transition network P , consisting of a directed graph with $2^L = 65,536$ nodes, and the weight of the edge P_{ij} denoting the probability of a transition occurring from node i to node j . Each node corresponds to a possible phenotype: we labeled nodes with labels l_i so that l_i was the binary representation of the phenotype at node i , and P_{ij} takes on the specific meaning of the probability of a transition from phenotype l_i to phenotype l_j . We made several restrictions on the structure of P . We allowed only transitions that change a given phenotype at one locus, so $P_{ij} = 0$ if $H(l_i, l_j) \neq 1$, where $H(b_1, b_2)$ is the Hamming distance between bitstrings b_1 and b_2 . Transitions that changed loci with value 1 to value 0 (steps back towards the C_3 state) were forbidden, so $P_{ij} = 0$ if $H(l_i, l_0) > H(l_j, l_0)$, where l_0 is the phenotypic string containing only zeroes. We assume that the possibility of events involving backwards steps, and multiple simultaneous trait acquisitions constitute second-order effects which will not strongly influence the inferred evolutionary dynamics.

Evolutionary trajectories

Given the transition network P , we modelled the evolutionary trajectories that may give rise to C_4 photosynthesis through the picture of a discrete analogue to a Brownian bridge, that is as a stochastic process on P with constrained start and end positions (*Revuz and Yor, 1999*). We enforced the start state of the process to be $l_{C_3} \equiv l_0 = 0 \dots 0$ (the phenotype string of all zeroes) and the end state, through the imposed structure of P , to be $l_{C_4} \equiv l_{2^L-1} = 1 \dots 1$ (the string of all ones). The dynamics of the process between these points consisted of L steps, with a phenotypic trait being acquired at each step, and a step from node i to node j occurring with probability P_{ij} .

Sampling intermediates

As many evolutionary trajectories may lead to the acquisition of the required phenotypic traits, we considered an ensemble of evolutionary trajectories for each transition network. Each member of this ensemble is started at l_{C_3} and allowed to step across the network according to probabilities P .

To compare the dynamics of a given transition network to the properties of observed biological intermediates, we pictured this ensemble of trajectories as a modification of a hidden Markov model (HMM [Rabiner, 1989]). At each timestep in each individual trajectory, the process may with some probability emit a signal to the observer, with that signal being simply l_i , the label of the node at which the process currently resides. Over an ensemble of trajectories, a set of randomly emitted signals is thus built up (Figure 1—figure supplement 4).

We define a compatibility function between two strings as

$$C(s, t) = \prod_{i=1}^L c(s_i, t_i) \quad (1)$$

$$c(s_i, t_i) = \begin{cases} 1 & \text{if } s_i = t_i \text{ or } s_i = 2 \text{ or } t_i = 2; \\ 0 & \text{otherwise.} \end{cases} \quad (2)$$

$C(s, t)$ thus returns 1 if a signal comprising string s could be responsible for observation t once some of the loci within s have been obscured: signal s is compatible with observation t .

Likelihood of observing biological data

We wish to compute the likelihood of observing biological data B given a transition network P . Under our model, this likelihood is calculated by considering the compatibility of randomly emitted signals from processes supported by P with the observed data B . We write

$$\mathcal{L}(P | B) = \prod_i \sum_{\text{chains } x} \sum_{\text{signals } s} \mathbb{P}_{\text{chain}}(x | P) \mathbb{P}_{\text{emission}}(s | x) C(s, B_i) \quad (3)$$

Here, $\mathbb{P}_{\text{chain}}(x | P)$ is the probability of specific trajectory x arising on network P , $\mathbb{P}_{\text{emission}}(s | x)$ is the probability that trajectory x emits signal s , and $C(s, B_i)$ gives the compatibility of signal s with intermediate state B_i . The term within the product operator thus describes the probability that evolutionary dynamics on network P give rise to a signal that is compatible with species B_i , with the overall likelihood being the product of this probability over all observed species.

Simulation

The uniform and random nature of signal emission means that $\mathbb{P}_{\text{emission}}(s | x)$ is a constant if signal s can be emitted from trajectory x , and zero otherwise. Our simulation approach only produces signals which can be emitted from the trajectory under consideration, so $\mathbb{P}_{\text{emission}}(s | x)$ will always take the same constant value (which depends on the probability of signal emissions). As we will be considering ratios of network likelihoods and will not be concerned with absolute likelihoods we will ignore this term henceforth. For each network P we simulate an ensemble of N_{chain} trajectories and, for each node encountered throughout this ensemble, we record compatibilities with each of the biologically observed intermediates. We sum these compatibilities over the ensemble, obtaining $\sum_{\text{chains } x} \mathbb{P}_{\text{chain}}(x | P) C(s, B_i)$. A network that does not encounter any node compatible with a particular intermediate will thus be assigned zero likelihood; networks that encounter compatible nodes many times will be assigned high likelihoods.

For each transition network, we simulated $N_{\text{chain}} = 2 \times 10^4$ individual trajectories running from C_3 to C_4 . This value was chosen after preliminary investigations to analyse the ability of trajectory ensembles to broadly sample available paths on networks.

Bayesian MCMC over compatible networks

Given uninformative prior knowledge about the evolutionary dynamics leading to C_4 photosynthesis (specifically, our prior involves each possible transition from a given node being assigned equal probability), we aimed to build a posterior distribution over a suitable description of the evolutionary dynamics. We represented the dynamics supported on a network P through a matrix π , where $\pi_{i,n}$

describes the probability that acquisition of trait i occurs at the n th step in an evolutionary trajectory. The values of matrix $\pi_{i,n}$ were built up from sampling over the ensemble of trajectories simulated on P .

We used Bayesian MCMC to sample networks based on their associated likelihood values (Wasserman, 2004). At each iteration, we perturbed the transition probability of the current network P a small amount (see below) to yield a new trial network P' . We calculated $\mathcal{L}(P' | B)$ and accepted P as the new network if $\frac{\mathcal{L}(P' | B)}{\mathcal{L}(P | B)} > r$, where r was taken from $\mathcal{U}(0,1)$. For practical reasons we implemented this scheme using log-likelihoods.

The perturbations we applied to transition probabilities are Normally distributed in logarithmic space: for each edge w_{ij} we used $w'_{ij} = \exp(\ln w_{ij} + \mathcal{N}(0, \sigma^2))$. To show that this scheme obeys detailed balance, consider two states A and A' , for simplicity described by a one-dimensional scalar quantity. Consider the proposed move from A when Δ is the result of the random draw. This proposal is $A \rightarrow A'$ if $A' = \exp(\ln A + \Delta) = Ae^\Delta$, implying that $A = A'e^{-\Delta}$. The probability of proposing move $A \rightarrow A'$ is thus $\mathcal{N}(x = \Delta | 0, \sigma^2)$, and the probability of proposing $A \rightarrow A'$ is $\mathcal{N}(x = -\Delta | 0, \sigma^2)$. By the symmetry of the Normal distribution, these two probabilities are equal.

We started each MCMC run with a randomly initialised transition matrix. We allowed 2×10^4 burn-in steps then sampled over a further 2×10^5 steps. The value $\sigma = 0.1$ was chosen for the perturbation kernel. These values were chosen through an initial investigation to analyse the convergence of MCMC runs under different parameterisations. We performed 40 MCMC runs for each experiment and confirmed that the resulting posterior distributions had converged and yielded consistent results.

Summary dynamics matrices

We report the posterior distributions $\mathbb{P}(\pi_{i,n})$ inferred from sampling compatible networks as above. In the coarse-grained time representation, we use $\pi_{i,n}^{CG} = \mathbb{P}\left(\sum_{n=1+4(n'-1)}^{4n'} \pi_{i,n}\right)$, summing over sets of ordinals of size 4.

We used the transition network P , rather than a more coarse-grained representation of the evolutionary dynamics (e.g., the summary matrices π), as the fundamental element within our simulations so as not to discard possible details that would be lost in a coarse-grained approach – for example, the presence of multiple distinct pathways, which may be averaged over in a summary matrix.

Proofs of principle

To verify our approach, we constructed artificial data sets, consisting of sets of strings in which phenotypic traits were acquired in a single ordering. Specifically, $\pi_{i,n} = \delta_{i,n}$, so the first step always resulted in acquiring the first trait, and so on. To test the approach in a pleiotropic setting, where multiple traits were acquired simultaneously, we also constructed data sets where traits were acquired at only four timesteps, each corresponding to the simultaneous acquisition of four traits. We subjected these datasets to our inferential machinery with all data intact, and with 50% of data points occluded, to determine the sensitivity and robustness of our approach (Figure 2A–B). The approach accurately determines the ordering of events in both the bare and occluded cases and assigns very similar posterior probability distributions to the ordering of those traits acquired simultaneously.

Comparing the evolution of multiple C_4 sub-types

To compare the pathways generating C_4 in monocots and eudicots, and in NADP-ME and NAD-ME sub-type lineages, we performed inference on two data sets: B_1 and B_2 , each comprising phenotype measurements from one of the groups of interest. We reported the posteriors on the resulting summary dynamics $\mathbb{P}(\pi_{i,n})$ as before, and for the principal components analysis (PCA) we sampled 10^3 summary dynamic matrices $\pi_{i,n}$ from the inferred posterior distribution during the Bayesian MCMC procedure, and performed PCA on these sampled matrices.

Predictions

When a simulated chain encountered a phenotypic node compatible with a given biological intermediate, the values of traits corresponding to missing data in the biological data were recorded. These recorded values, sampled over the sampled set of networks, allowed us to place probabilities on the values of biologically unobserved traits inferred from the encounters of compatible dynamics with the corresponding phenotypic possibilities. For example, if 70% of paths on network P pass through point 101 and

30% pass through point 001, we infer a 70% probability that the missing trait in biological intermediate 201 takes the value 1. Predictions were presented if the inferred probability of a '1' value was >75% (predicting a '1') or <25% (predicting a '0'). If one of these inequalities held and the limiting value fell outside one standard deviation of the inferred probability (i.e., for mean μ and standard deviation σ , $\mu > 0.75$ and $\mu - \sigma > 0.75$ [predicting a '1'] or $\mu > 0.25$ and $\mu + \sigma < 0.25$ [predicting a '0']), the prediction was presented as 'strict'.

Acquisition ordering and evidence against a single pathway

We used a dynamic programming approach to explore whether a deterministic sequence of events, with a trait T_n always being acquired at timestep n ($\pi_{i,n} = \delta_{T_n,n}$), was compatible with the biological data. Performing an exhaustive search over sequences of single transitions that were compatible with the observed data, we identified several such sequences that accounted for all but one trait acquisition, but no single sequence exists that accounts for all the data.

Contingent trait acquisition

To explore the possibility of multiple traits being acquired simultaneously, we tracked acquisition probabilities for later traits given that a certain trait was acquired first. This tracking was performed over all sampled compatible networks, building up 'contingent' acquisition tables γ with the i, j th element given by $\mathbb{P}(\pi_{j,2} | \pi_{i,1} = 1), j \neq i$. If a pair of traits i and j were acquired simultaneously, we would expect γ_{ij} and γ_{ji} to both be higher than expected in the non-contingent case (as j should always appear to be immediately acquired after i and vice versa).

Quantitative real-time PCR (qPCR)

RNA was extracted from mature leaves of six *Flaveria* species as part of the One Thousand Plants Consortium (www.onekp.com), using the hot acid phenol protocol as described by **Johnson et al. (2012)** (protocol no. 12). cDNA was synthesised from 0.5 μ g RNA using Superscript II (Life Technologies, Glasgow, U.K.) following manufacturer's instructions. An oligo dT primer (Roche, Basel, Switzerland) was used to selectively transcribe polyadenylated transcripts. To each RNA sample, 1 fmol GUS transcript was added for use as an exogenous control or 'RNA spike', against which measured transcript abundance was normalised as described by **Smith et al. (2003)**.

qPCR was performed as described by **Bustin (2000)** using the DNA-binding marker SYBR Green (Sigma Aldrich, St. Louis, MO) according to manufacturer's instructions. Primers were designed using cDNA sequences for *Flaveria* species available at Genbank (<http://www.ncbi.nlm.nih.gov/genbank>) and synthesised by Life Technologies. Amplification was performed using a Rotor-Gene Q instrument (Qiagen, Hilden, Germany), using the following cycling parameters: 94°C for 2 min, followed by 40 cycles at 94°C for 20 s, 60°C for 30 s, 72°C for 30 s, followed by a 5 min incubation at 72°C. Relative transcript abundance was calculated as described by **Livak and Schmittgen (2001)**.

Acknowledgements

We thank S Kelly, JA Langdale, H Griffiths, and N Jones for advice.

Additional information

Funding

Funder	Author
Biotechnology and Biological Sciences Research Council	Ben P Williams, Iain G Johnston, Julian M Hibberd
International Rice Research Institute	Sarah Covshoff

The funders had no role in study design, data collection and interpretation, or the decision to submit the work for publication.

Author contributions

BPW, IGJ, Conception and design, Acquisition of data, Analysis and interpretation of data, Drafting or revising the article; SC, Acquisition of data, Analysis and interpretation of data, Drafting or revising the article; JMH, Conception and design, Analysis and interpretation of data, Drafting or revising the article

References

- Abramoff MD**, Magalhaes PJ, Ram SJ. 2004. Image processing with ImageJ. *Biophotonics Int* **11**:36–42.
- Adams CA**, Leung F, Sun SSM. 1986. Molecular properties of phosphoenolpyruvate carboxylase from C₃, C₃-C₄ intermediate, and C₄ *Flaveria* species. *Planta* **167**:218–25. doi: [10.1007/BF00391418](https://doi.org/10.1007/BF00391418).
- Akyildiz M**, Gowik U, Engelmann S, Koczor M, Streubel M, Westhoff P. 2007. Evolution and function of a cis-regulatory module for mesophyll-specific gene expression in the C₄ dicot *Flaveria trinervia*. *Plant Cell* **19**:3391–402. doi: [10.1105/tpc.107.053322](https://doi.org/10.1105/tpc.107.053322).
- Aubry S**, Brown NJ, Hibberd JM. 2011. The role of proteins in C₃ plants prior to their recruitment into the C₄ pathway. *J Exp Bot* **62**:3049–59. doi: [10.1093/jxb/err012](https://doi.org/10.1093/jxb/err012).
- Beebe DU**, Evert RF. 1990. The morphology and anatomy of the leaf of *Moricandia arvensis* (L.) DC. (Brassicaceae). *Bot Gaz* **151**:184–203. doi: [10.1086/337818](https://doi.org/10.1086/337818).
- Brown NJ**, Newell CA, Stanley S, Chen JE, Perrin AJ, Kajala K, et al. 2011. Independent and parallel recruitment of preexisting mechanisms underlying C₄ photosynthesis. *Science* **331**:1436–9. doi: [10.1126/science.1201248](https://doi.org/10.1126/science.1201248).
- Brown RH**, Hattersley PW. 1989. Leaf anatomy of C₃-C₄ species as related to evolution of C₄ photosynthesis. *Plant Physiol* **91**:1543–50. doi: [10.1104/pp.91.4.1543](https://doi.org/10.1104/pp.91.4.1543).
- Bruhl JJ**, Perry S. 1995. Photosynthetic pathway-related ultrastructure of C₃, C₄ and C₃-like C₃-C₄ intermediate sedges (Cyperaceae), with special reference to *Eleocharis*. *Aust J Plant Physiol* **22**:521. doi: [10.1071/PP9950521](https://doi.org/10.1071/PP9950521).
- Bustin SA**. 2000. Absolute quantification of mRNA using real-time reverse transcription polymerase chain reaction assays. *J Mol Endocrinol* **25**:169–93. doi: [10.1677/jme.0.0250169](https://doi.org/10.1677/jme.0.0250169).
- Casati P**, Fresco AG, Andreo CS, Drincovich MF. 1999. An intermediate form of NADP-malic enzyme from the C₃-C₄ intermediate species *Flaveria floridana*. *Plant Science* **147**:101–9. doi: [10.1016/S0168-9452\(99\)00101-6](https://doi.org/10.1016/S0168-9452(99)00101-6).
- Cheng SH**, Moore BD, Edwards GE, Ku MS. 1988. Photosynthesis in *Flaveria brownii*, a C₄-like species: leaf anatomy, characteristics of CO₂ exchange, compartmentation of photosynthetic enzymes, and metabolism of CO₂. *Plant Physiol* **87**:867–73. doi: [10.1104/pp.87.4.867](https://doi.org/10.1104/pp.87.4.867).
- Christin P-A**, Osborne CP, Chatelet DS, Columbus JT, Besnard G, Hodkinson TR, et al. 2013. Anatomical enablers and the evolution of C₄ photosynthesis in grasses. *Proc Natl Acad Sci USA* **110**:1381–6. doi: [10.1073/pnas.1216777110](https://doi.org/10.1073/pnas.1216777110).
- Christin P-A**, Osborne CP, Sage RF, Arakaki M, Edwards EJ. 2011b. C₄ eudicots are not younger than C₄ monocots. *J Exp Bot* **62**:3171–81. doi: [10.1093/jxb/err041](https://doi.org/10.1093/jxb/err041).
- Christin P-A**, Sage TL, Edwards EJ, Ogburn RM, Khoshravesh R, Sage RF. 2011a. Complex evolutionary transitions and the significance of C₃-C₄ intermediate forms of photosynthesis in Molluginaceae. *Evolution* **65**:643–60. doi: [10.1111/j.1558-5646.2010.01168.x](https://doi.org/10.1111/j.1558-5646.2010.01168.x).
- Christin P**, Besnard G, Samaritani E, Duvall M, Hodkinson T, Savolainen V, et al. 2008. Oligocene CO₂ decline promoted C₄ photosynthesis in grasses. *Curr Biol* **18**:37–43. doi: [10.1016/j.cub.2007.11.058](https://doi.org/10.1016/j.cub.2007.11.058).
- Christin P**, Salamin N, Savolainen V, Duvall M, Besnard G. 2007. C₄ photosynthesis evolved in grasses via parallel adaptive genetic changes. *Curr Biol* **17**:1241–7. doi: [10.1016/j.cub.2007.06.036](https://doi.org/10.1016/j.cub.2007.06.036).
- Devi MT**, Raghavendra AS. 1993. Partial reduction in activities of photorespiratory enzymes in C₃-C₄ intermediates of *Alternanthera* and *Parthenium*. *J Exp Bot* **44**:779–84. doi: [10.1093/jxb/44.4.779](https://doi.org/10.1093/jxb/44.4.779).
- Devi MT**, Rajagopalan AV, Raghavendra AS. 1995. Predominant localization of mitochondria enriched with glycine-decarboxylating enzymes in bundle sheath cells of *Alternanthera tenella*, a C₃-C₄ intermediate species. *Plant Cell Environ* **18**:589–94. doi: [10.1111/j.1365-3040.1995.tb00559.x](https://doi.org/10.1111/j.1365-3040.1995.tb00559.x).
- Edwards EJ**, Osborne CP, Stromberg CAE, Smith SA, C₄ grasses consortium. 2010. The origins of C₄ grasslands: integrating evolutionary and ecosystem science. *Science* **328**:587–91. doi: [10.1126/science.1177216](https://doi.org/10.1126/science.1177216).
- Furbank RT**. 2011. Evolution of the C₄ photosynthetic mechanism: are there really three C₄ acid decarboxylation types? *J Exp Bot* **62**:3103–8. doi: [10.1093/jxb/err080](https://doi.org/10.1093/jxb/err080).
- Gavrilets S**. 1997. Evolution and speciation on holey adaptive landscapes. *Trends Ecol Evol* **12**:307–12. doi: [10.1016/S0169-5347\(97\)01098-7](https://doi.org/10.1016/S0169-5347(97)01098-7).
- Goldstein L**, Ray T, Kestler D, Mayne B, Brown R, Black C. 1976. Biochemical characterization of panicum species which are intermediate between C₃ and C₄ photosynthesis plants. *Plant Sci* **6**:85–90. doi: [10.1016/0304-4211\(76\)90140-1](https://doi.org/10.1016/0304-4211(76)90140-1).
- Gowik U**, Brautigam A, Weber KL, Weber APM, Westhoff P. 2011. Evolution of C₄ photosynthesis in the genus *Flaveria*: how many and which genes does it take to make C₄? *Plant Cell* **23**:2087–105. doi: [10.1105/tpc.111.086264](https://doi.org/10.1105/tpc.111.086264).
- Griffiths H**, Weller G, Toy LFM, Dennis RJ. 2013. You're so vein: bundle sheath physiology, phylogeny and evolution in C₃ and C₄ plants. *Plant Cell Environ* **36**:249–61. doi: [10.1111/j.1365-3040.2012.02585.x](https://doi.org/10.1111/j.1365-3040.2012.02585.x).
- Hatch MD**, Kagawa T, Craig S. 1975. Subdivision of C₄ pathway species based on differing C₄ acid decarboxylating systems and ultrastructural features. *Aust J Plant Physiol* **2**:111–28. doi: [10.1071/PP9750111](https://doi.org/10.1071/PP9750111).
- Hattersley PW**. 1984. Characterization of C₄ type leaf anatomy in grasses (Poaceae). Mesophyll: bundle sheath area ratios. *Ann Bot* **53**:163–80.
- Hattersley PW**, Stone NE. 1986. Photosynthetic enzyme activities in the C₃-C₄ intermediate *Neurachne minor*. *Aust J Plant Physiol* **13**:399. doi: [10.1071/PP9860399](https://doi.org/10.1071/PP9860399).
- Heckman D**, Schulze S, Denton A, Gowik U, Westhoff P, Weber APM, et al. 2013. Predicting C₄ photosynthesis evolution: modular, individually adaptive steps on a Mount Fuji fitness landscape. *Cell* **153**:1579–88. doi: [10.1016/j.cell.2013.04.058](https://doi.org/10.1016/j.cell.2013.04.058).
- Hibberd JM**, Sheehy JE, Langdale JA. 2008. Using C₄ photosynthesis to increase the yield of rice—rationale and feasibility. *Curr Opin Plant Biol* **11**:228–31. doi: [10.1016/j.pbi.2007.11.002](https://doi.org/10.1016/j.pbi.2007.11.002).
- Hill RC**, Egydio de Carvalho C, Salogiannis J, Schlager B, Pilgrim D, Haag ES. 2006. Genetic flexibility in the convergent evolution of hermaphroditism in *Caenorhabditis* nematodes. *Dev Cell* **10**:531–8. doi: [10.1016/j.devcel.2006.02.002](https://doi.org/10.1016/j.devcel.2006.02.002).

- Holaday AS**, Black CC. 1981. Comparative characterization of phosphoenolpyruvate carboxylase in C₃, C₄, and C₃-C₄ intermediate *Panicum* species. *Plant Physiol* **67**:330–4. doi: [10.1104/pp.67.2.330](https://doi.org/10.1104/pp.67.2.330).
- Holaday AS**, Lee KW, Chollet R. 1984. C₃-C₄ Intermediate species in the genus *Flaveria*: leaf anatomy, ultrastructure, and the effect of O₂ on the CO₂ compensation concentration. *Planta* **160**:25–32. doi: [10.1007/BF00392462](https://doi.org/10.1007/BF00392462).
- Holaday AS**, Shieh Y-J, Lee KW, Chollet R. 1981. Anatomical, ultrastructural and enzymic studies of leaves of *Moricandia arvensis*, a C₃-C₄ intermediate species. *Biochim Biophys Acta* **637**:334–41. doi: [10.1016/0005-2728\(81\)90172-9](https://doi.org/10.1016/0005-2728(81)90172-9).
- Hylton CM**, Rawsthorne S, Smith AM, Jones DA, Woolhouse HW. 1988. Glycine decarboxylase is confined to the bundle-sheath cells of leaves of C₃-C₄ intermediate species. *Planta* **175**:452–9. doi: [10.1007/BF00393064](https://doi.org/10.1007/BF00393064).
- Johnson MTJ**, Carpenter EJ, Tian Z, Bruskiwich R, Burriss JN, Carrigan CT, et al. 2012. Evaluating methods for isolating total RNA and predicting the success of sequencing phylogenetically diverse plant transcriptomes. *PLOS ONE* **7**:e50226. doi: [10.1371/journal.pone.0050226](https://doi.org/10.1371/journal.pone.0050226).
- Kajala K**, Brown NJ, Williams BP, Borrill P, Taylor LE, Hibberd JM. 2012. Multiple *Arabidopsis* genes primed for recruitment into C₄ photosynthesis. *Plant J* **69**:47–56. doi: [10.1111/j.1365-313X.2011.04769.x](https://doi.org/10.1111/j.1365-313X.2011.04769.x).
- Keeley JE**. 1999. Photosynthetic pathway diversity in a seasonal pool community. *Funct Ecol* **13**:106–18. doi: [10.1046/j.1365-2435.1999.00294.x](https://doi.org/10.1046/j.1365-2435.1999.00294.x).
- Kennedy RA**, Eastburn JL, Jensen KG. 1980. C₃-C₄ Photosynthesis in the genus *Mollugo*: structure, physiology and evolution of intermediate characteristics. *Am J Bot* **67**:1207–17. doi: [10.2307/2442363](https://doi.org/10.2307/2442363).
- Khoshravesh R**, Hossein A, Sage TL, Nordenstam B, Sage RF. 2012. Phylogeny and photosynthetic pathway distribution in *Anticharis* Endl. (Scrophulariaceae). *J Exp Bot* **63**:5645–58. doi: [10.1093/jxb/ers218](https://doi.org/10.1093/jxb/ers218).
- Kidwell SM**, Holland SM. 2002. The quality of the fossil record: implications for evolutionary analyses. *Ann Rev Ecol Syst* **33**:561–88. doi: [10.1146/annurev.ecolsys.33.030602.152151](https://doi.org/10.1146/annurev.ecolsys.33.030602.152151).
- Koteyeva NK**, Voznesenskaya EV, Roalson EH, Edwards GE. 2010. Diversity in forms of C₄ in the genus *Cleome* (Cleomaceae). *Ann Bot* **107**:269–83. doi: [10.1093/aob/mcq239](https://doi.org/10.1093/aob/mcq239).
- Kozmik Z**, Ruzickova J, Jonasova K, Matsumoto Y, Vopalensky P, Kozmikova I, et al. 2008. Assembly of the cnidarian camera-type eye from vertebrate-like components. *Proc Natl Acad Sci USA* **105**:8989–93. doi: [10.1073/pnas.0800388105](https://doi.org/10.1073/pnas.0800388105).
- Ku MSB**, Edwards GE. 1978. Photosynthetic efficiency of *Panicum hians* and *Panicum milioides* in relation to C₃ and C₄ plants. *Plant Cell Physiol* **19**:665–75.
- Ku MSB**, Edwards GE, Kanai R. 1976. Distribution of enzymes related to C₃ and C₄ pathway of photosynthesis between mesophyll and bundle sheath cells of *Panicum hians* and *Panicum milioides*. *Plant Cell Physiol* **17**:615–20.
- Ku MSB**, Monson RK, Littlejohn RO, Nakamoto H, Fisher DB, Edwards GE. 1983. Photosynthetic characteristics of C₃-C₄ intermediate *Flaveria* species¹: I. leaf anatomy, photosynthetic responses to O₂ and CO₂, and activities of key enzymes in the C₃ and C₄ Pathways. *Plant Physiol* **71**:944–8. doi: [10.1104/pp.71.4.944](https://doi.org/10.1104/pp.71.4.944).
- Ku MSB**, Wu J, Dai Z, Scott RA, Chu C, Edwards GE. 1991. Photosynthetic and photorespiratory characteristics of *Flaveria* species. *Plant Physiol* **96**:518–28. doi: [10.1104/pp.96.2.518](https://doi.org/10.1104/pp.96.2.518).
- Langdale JA**. 2011. C₄ cycles: past, present, and future research on C₄ photosynthesis. *Plant Cell* **23**:3879–92. doi: [10.1105/tpc.111.092098](https://doi.org/10.1105/tpc.111.092098).
- Livak KJ**, Schmittgen TD. 2001. Analysis of relative gene expression data using real-time quantitative PCR and the 2(-Delta Delta C(T)) method. *Methods* **25**:402–8. doi: [10.1006/meth.2001.1262](https://doi.org/10.1006/meth.2001.1262).
- Lobkovsky AE**, Wolf YI, Koonin EV. 2011. Predictability of evolutionary trajectories in fitness landscapes. *PLOS Comput Biol* **7**:e1002302. doi: [10.1371/journal.pcbi.1002302](https://doi.org/10.1371/journal.pcbi.1002302).
- McKown AD**, Dengler NG. 2007. Key innovations in the evolution of Kranz anatomy and C₄ vein pattern in *Flaveria* (Asteraceae). *Am J Bot* **94**:382–99. doi: [10.3732/ajb.94.3.382](https://doi.org/10.3732/ajb.94.3.382).
- McKown AD**, Moncalvo J-M, Dengler NG. 2005. Phylogeny of *Flaveria* (Asteraceae) and inference of C₄ photosynthesis evolution. *Am J Bot* **92**:1911–28. doi: [10.3732/ajb.92.11.1911](https://doi.org/10.3732/ajb.92.11.1911).
- Moore AO**, Heard SB. 2013. Inferring evolutionary process from phylogenetic tree shape. *Q Rev Biol* **72**:31–54. doi: [10.1086/419657](https://doi.org/10.1086/419657).
- Moore BD**, Franceschi VR, Cheng S-H, Wu J, Ku MSB. 1987. Photosynthetic characteristics of the C₃-C₄ intermediate *Parthenium hysterophorus*. *Plant Physiol* **85**:978–83. doi: [10.1104/pp.85.4.978](https://doi.org/10.1104/pp.85.4.978).
- Muhaidat R**, Sage TL, Frohlich MW, Dengler NG, Sage RF. 2011. Characterization of C₃-C₄ intermediate species in the genus *Heliotropium* L. (Boraginaceae): anatomy, ultrastructure and enzyme activity. *Plant Cell Environ* **34**:1723–36. doi: [10.1111/j.1365-3040.2011.02367.x](https://doi.org/10.1111/j.1365-3040.2011.02367.x).
- Osborne CP**, Sack L. 2012. Evolution of C₄ plants: a new hypothesis for an interaction of CO₂ and water relations mediated by plant hydraulics. *Philos Trans R Soc Lond B Biol Sci* **367**:583–600. doi: [10.1098/rstb.2011.0261](https://doi.org/10.1098/rstb.2011.0261).
- P'yankov VI**, Voznesenskaya EV, Kondratschuk AV, Black CC. 1997. A comparative anatomical and biochemical analysis in *Salsola* (Chenopodiaceae) species with and without a Kranz type leaf anatomy: a possible reversion of C₄ to C₃ photosynthesis. *Am J Bot* **84**:597.
- Rabiner L**. 1989. A tutorial on hidden Markov models and selected applications in speech recognition. *Proc IEEE* **77**:257–86. doi: [10.1109/5.18626](https://doi.org/10.1109/5.18626).
- Rajendrudu G**, Prasad JSR, Das VSR. 1986. C₃-C₄ intermediate species in *Alternanthera* (Amaranthaceae)¹: leaf anatomy, CO₂ compensation point, net CO₂ exchange and activities of photosynthetic enzymes. *Plant Physiol* **80**:409–14. doi: [10.1104/pp.80.2.409](https://doi.org/10.1104/pp.80.2.409).
- Rathnam CKM**, Chollet R. 1978. CO₂ donation by malate and aspartate reduces photorespiration in *Panicum milioides*, A C₃-C₄ intermediate species. *Biochem Biophys Res Comm* **85**:801–8. doi: [10.1016/0006-291X\(78\)91233-0](https://doi.org/10.1016/0006-291X(78)91233-0).

- Rathnam CKM**, Chollet R. 1979. Photosynthetic carbon metabolism in *Panicum milioides*, a C₃-C₄ intermediate species: evidence for a limited C₄ dicarboxylic acid pathway of photosynthesis. *Biochim Biophys Acta* **548**:500–19. doi: [10.1016/0005-2728\(79\)90061-6](https://doi.org/10.1016/0005-2728(79)90061-6).
- Rawsthorne S**, Hylton CM, Smith AM, Woolhouse HW. 1988. Photorespiratory metabolism and immunogold localization of photorespiratory enzymes in leaves of C₃ and C₃-C₄ intermediate species of *Moricandia*. *Planta* **173**:298–308. doi: [10.1007/BF00401016](https://doi.org/10.1007/BF00401016).
- Rawsthorne S**, Morgan CL, O'Neill CM, Hylton CM, Jones DA, Freen ML. 1998. Cellular expression pattern of the glycine decarboxylase P protein in leaves of an intergeneric hybrid between the C₃-C₄ intermediate species *Moricandia nitens* and the C₃ species *Brassica napus*. *Theoret App Genet* **96**:922–7. doi: [10.1007/s001220050821](https://doi.org/10.1007/s001220050821).
- Revuz D**, Yor M. 1999. *Continuous Martingales and Brownian Motion*. Springer.
- Rosche E**, Streubel M, Westhoff P. 1994. Primary structure of the photosynthetic pyruvate orthophosphate dikinase of the C₃ plant *Flaveria pringlei* and expression analysis of pyruvate orthophosphate dikinase sequences in C₃, C₃-C₄ and C₄ *Flaveria* species. *Plant Mol Biol* **26**:763–9. doi: [10.1007/BF00013761](https://doi.org/10.1007/BF00013761).
- Roweis S**. 1998. Em algorithms for PCA and SPCA. *Advances in Neural Information Processing Systems*. Cambridge, MA: MIT Press. p. 626–32.
- Sage RF**, Christin P-A, Edwards EJ. 2011a. The C₄ plant lineages of planet Earth. *J Exp Bot* **62**:3155–69. doi: [10.1093/jxb/err048](https://doi.org/10.1093/jxb/err048).
- Sage RF**, Sage TL, Kocacinar F. 2012. Photorespiration and the evolution of C₄ photosynthesis. *Annu Rev Plant Biol* **63**:19–47. doi: [10.1146/annurev-arplant-042811-105511](https://doi.org/10.1146/annurev-arplant-042811-105511).
- Sage TL**, Sage RF, Vogan PJ, Rahman B, Johnson DC, Oakley JC, et al. 2011b. The occurrence of C₂ photosynthesis in *Euphorbia* subgenus *Chamaesyce* (Euphorbiaceae). *J Exp Bot* **62**:3183–95. doi: [10.1093/jxb/err059](https://doi.org/10.1093/jxb/err059).
- Santos JC**, Coloma LA, Cannatella DC. 2003. Multiple, recurring origins of aposematism and diet specialization in poison frogs. *Proc Natl Acad Sci USA* **100**:12792–7. doi: [10.1073/pnas.2133521100](https://doi.org/10.1073/pnas.2133521100).
- Sayre RT**, Kennedy RA, Pringnitz DJ. 1979. Photosynthetic enzyme activities and localization in *Mollugo verticillata* populations differing in the levels of C₃ and C₄ cycle operation. *Plant Physiol* **64**:293–9. doi: [10.1104/pp.64.2.293](https://doi.org/10.1104/pp.64.2.293).
- Slack CR**, Hatch MD. 1967. Comparative studies on the activity of carboxylases and other enzymes in relation to the new pathway of photosynthetic carbon dioxide fixation in tropical grasses. *Biochem J* **103**:660–5. doi: [10.1042/bj1030660](https://doi.org/10.1042/bj1030660).
- Smith RD**, Brown B, Ikononi P, Schechter AN. 2003. Exogenous reference RNA for normalization of real-time quantitative PCR. *BioTechniques* **34**:88–91. doi: [11200322](https://doi.org/10.11200322).
- Steiner CC**, Römpler H, Boettger LM, Schöneberg T, Hoekstra HE. 2009. The genetic basis of phenotypic convergence in beach mice: similar pigment patterns but different genes. *Mol Biol Evol* **26**:35–45. doi: [10.1093/molbev/msn218](https://doi.org/10.1093/molbev/msn218).
- Ueno O**, Bang SW, Wada Y, Kondo A, Ishihara K, Kaneko Y, et al. 2003. Structural and biochemical dissection of photorespiration in hybrids differing in genome constitution between *Diploptaxis tenuifolia* (C₃-C₄) and Radish (C₃). *Plant Physiol* **132**:1550–9. doi: [10.1104/pp.103.021329](https://doi.org/10.1104/pp.103.021329).
- Ueno O**, Wada Y, Wakai M, Bang SW. 2006. Evidence from photosynthetic characteristics for the hybrid origin of *Diploptaxis muralis* from a C₃-C₄ intermediate and a C₃ species. *Plant Biol* **8**:253–9. doi: [10.1055/s-2005-873050](https://doi.org/10.1055/s-2005-873050).
- Vicentini A**, Barber JC, Aliscioni SS, Giussani LM, Kellogg EA. 2008. The age of the grasses and clusters of origins of C₄ photosynthesis. *Glob Change Biol* **14**:2963–77. doi: [10.1111/j.1365-2486.2008.01688.x](https://doi.org/10.1111/j.1365-2486.2008.01688.x).
- Vogan PJ**, Frohlich MW, Sage RF. 2007. The functional significance of C₃-C₄ intermediate traits in *Heliotropium* L. (Boraginaceae): gas exchange perspectives. *Plant Cell Environ* **30**:1337–45. doi: [10.1111/j.1365-3040.2007.01706.x](https://doi.org/10.1111/j.1365-3040.2007.01706.x).
- Voznesenskaya EV**, Artyusheva EG, Franceschi VR, Pyankov VI, Kiirats O, Ku M, et al. 2001. *Salsola arbusculiformis*, a C₃-C₄ Intermediate in Salsoleae (Chenopodiaceae). *Ann Bot* **88**:337–48. doi: [10.1006/anbo.2001.1457](https://doi.org/10.1006/anbo.2001.1457).
- Voznesenskaya EV**, Koteyeva NK, Chuong SDX, Ivanova AN, Barroca J, Craven LA, et al. 2007. Physiological, anatomical and biochemical characterisation of photosynthetic types in genus *Cleome* (Cleomaceae). *Funct Plant Biol* **34**:247. doi: [10.1071/FP06287](https://doi.org/10.1071/FP06287).
- Voznesenskaya EV**, Koteyeva NK, Edwards GE, Ocampo G. 2010. Revealing diversity in structural and biochemical forms of C₄ photosynthesis and a C₃-C₄ intermediate in genus *Portulaca* L. (Portulacaceae). *J Exp Bot* **61**:3647–62. doi: [10.1093/jxb/erq178](https://doi.org/10.1093/jxb/erq178).
- Wasserman L**. 2004. *All of statistics: a concise course in statistical inference*. Springer.
- Weinreich DM**, Watson RA, Chao L. 2005. Sign epistasis and genetic constraint on evolutionary trajectories. *Evolution* **59**:1165–74. doi: [10.1111/j.0014-3820.2005.tb01768.x](https://doi.org/10.1111/j.0014-3820.2005.tb01768.x).
- Whibley AC**, Langlade NB, Andalo C, Hanna AI, Bangham A, Thébaud C, et al. 2006. Evolutionary paths underlying flower color variation in *Antirrhinum*. *Science* **313**:963–6. doi: [10.1126/science.1129161](https://doi.org/10.1126/science.1129161).
- Williams BP**, Aubry S, Hibberd JM. 2012. Molecular evolution of genes recruited into C₄ photosynthesis. *Trends Plant Sci* **17**:213–20. doi: [10.1016/j.tplants.2012.01.008](https://doi.org/10.1016/j.tplants.2012.01.008).
- Wilson JS**, Williams KA, Forister ML, von Dohlen CD, Pitts JP. 2012. Repeated evolution in overlapping mimicry rings among North American velvet ants. *Nat Commun* **3**:1272. doi: [10.1038/ncomms2275](https://doi.org/10.1038/ncomms2275).
- Wiludda C**, Schulze S, Gowik U, Engelmann S, Koczor M, Streubel M, et al. 2012. Regulation of the photorespiratory GLDPA gene in C₄ *Flaveria*: an intricate interplay of transcriptional and post-transcriptional processes. *Plant Cell* **24**:137–51. doi: [10.1105/tpc.111.093872](https://doi.org/10.1105/tpc.111.093872).
- Wittkopp PJ**, Williams BL, Selegue JE, Carroll SB. 2003. Drosophila pigmentation evolution: divergent genotypes underlying convergent phenotypes. *Proc Natl Acad Sci USA* **100**:1808–13. doi: [10.1073/pnas.0336368100](https://doi.org/10.1073/pnas.0336368100).
- Wright S**. 1932. The roles of mutation, inbreeding, crossbreeding and selection in evolution. *Proc Sixth Int Congr Genet* **1**:356–66.
- Zhu X-G**, Long SP, Ort DR. 2008. What is the maximum efficiency with which photosynthesis can convert solar energy into biomass? *Curr Opin Biotechnol* **19**:153–9. doi: [10.1016/j.copbio.2008.02.004](https://doi.org/10.1016/j.copbio.2008.02.004).